energies

MDPI

Article

Adaptive Band-Pass Filter and VMD-Esprit Based Multi-Mode Monitoring Method for Broadband Electromagnetic Oscillation in "Double High" Power Systems

Tie Zhong, Heling Yang, Cong Sun, Chuang Liu * and Junrui Chen

Department of Communication Engineering, Northeast Electric Power University, Jilin 132013, China
* Correspondence: victorliuchuang@163.com

Abstract: With the development of new power systems with high proportions of renewable energy and high proportions of power electronics equipment, the influence of broadband electromagnetic oscillations in power systems is becoming more and more significant. In order to better grasp the dynamic characteristics of broadband oscillations, a new adaptive band-pass filter and VMD-Esprit based multi-modal monitoring method is proposed for broadband electromagnetic oscillation in "double high" power systems. First, based on the mode frequency and amplitude information provided by FFT mode detection, the proposed adaptive band-pass filter adaptively sets the center frequency, bandwidth, and other parameters and extracts or separates the voltage/current signal in each frequency band. Second, the filtered signals are corrected and compensated, and then the VMD modal decomposition of each frequency band signal is combined with Esprit for parameter identification so as to obtain the waveform and parameter information of each mode. Finally, the separation, correction, and parameter identification of multi-mode broadband oscillation waveforms are carried out. The experimental results show that frequency division processing can reduce the computation and improve real-time performance. In the processing of signals in the frequency band, the center frequency, bandwidth, and other parameters can be adjusted adaptively under different conditions of single-mode composition or multi-mode composition, which improves the accuracy of VMD decomposition and increases the flexibility of signal processing. Meanwhile, it overcomes the defects such as the inaccuracy of traditional mode recognition, which provides a new idea for broadband electromagnetic oscillation analysis.

Keywords: multi-mode monitoring; broadband electromagnetic oscillation; adaptive band-pass filtering; VMD-Esprit; "double high" power system

check for updates

Citation: Zhong, T.; Yang, H.; Sun, C.; Liu, C.; Chen, J. Adaptive Band-Pass Filter and VMD-Esprit Based Multi-Mode Monitoring Method for Broadband Electromagnetic Oscillation in "Double High" Power Systems. *Energies* **2023**, *16*, 3110. https://doi.org/10.3390/en16073110

Academic Editor: Konstantin Suslov

Received: 17 February 2023
Revised: 3 March 2023
Accepted: 8 March 2023
Published: 29 March 2023

1. Introduction

At present, China is in the early stage of the new energy revolution, and renewable energy is replacing traditional fossil energy as the main source of energy supply [1]. By the end of 2020, the installed capacity of new energy power generation in China was about 2.2 billion kilowatts, of which the installed capacity of grid-connected wind power was about 280 million kilowatts, and the installed capacity of grid-connected solar power was about 250 million kilowatts, accounting for 12.8 and 11.5% respectively. At the same time, due to the particularity of the geographical distribution of the supply and the load demand for the new energy power generation, in order to realize the efficient and flexible transmission of electric energy from the new energy power station to the load, the long-distance high-voltage flexible DC transmission network is gradually forming, such as Zhangbei to Beijing [2,3]. By the end of 2020, China had built 17 UHV DC transmission lines [4,5]. The interaction between AC and DC systems [6] has become one of the most important factors determining the level of system security and stability. At the same time, with the progress and upgrading of various industries, DC terminals with excellent control by means of power electronic devices are continuously connected to the AC power grid [7,8].

All in all, with the development of a large number of new energy power generation grid connections, high voltage direct current transmission, and high power direct current load, the proportion of power electronics in each part of the power system 'source-network-load' is becoming higher and higher [9]. Power electronic equipment is widely used in power generation, transmission, distribution, and power consumption of power systems. It has become an important trend in power systems that traditional electromechanical-electromagnetic conversion equipment, such as synchronous generators, are gradually replaced by power electronic equipment.

With the development of new energy power generation technology, power systems have widely transitioned to power electronics equipment; that is also why power systems appear to have "double high" characteristics [10,11] (i.e., high proportions of new energy power generation and high proportions of power electronics equipment). With these characteristics becoming more and more prominent, broadband oscillation has become more frequent as a result. According to incomplete statistics, there have been many serious oscillation events at home and abroad in recent years. In addition, the range of frequency ranges from several Hz to several thousand Hz. For example, this synchronous resonance occurs in the Hebei Guyuan wind power-series compensation system [12,13], and the frequency varies from 3 to 12 Hz. In 2015, the subsynchronous oscillation phenomenon occurred at the Xinjiang Hami wind farm [14,15], and the oscillation frequency changed in a large range (10~40 Hz), with significant time-varying characteristics; this synchronous oscillation occurs in the Ajo wind farm-series compensation system in Texas [16], and the oscillation frequency is about 20 Hz. In the high-frequency harmonic oscillation of the Borwin wind power-flexible direct transmission system in the North Sea of Europe [17], the oscillation frequency range is between 250~350 Hz. For the safe and stable operation of power systems, broadband oscillation is becoming a serious threat.

For various broadband oscillation phenomena, although there are differences in mechanism and manifestation, there is a unified form in the mathematical model. Therefore, they have many common characteristics, such as a wide frequency range, complex influencing factors, and large-scale time-varying characteristics. Moreover, the oscillation phenomenon often starts from small signal negative damping divergence and ends in nonlinear continuous oscillation. The broadband oscillation that power electronics equipment mainly participates in is the dynamic interaction between multiple converters, renewable energy units, and AC/DC power grids. It is essentially different from the traditional electromechanical (low frequency) oscillation and traditional subsynchronous resonance/oscillation dominated by the inertia and shafting dynamics of rotating units. From the above analysis, it can be seen that the electromagnetic signal of the power system presents the characteristics of multi-mode superposition, time-varying, time-space distribution, and so on. In order to reduce the unnecessary loss caused by broadband electromagnetic oscillation, the power system can use a real-time monitoring system to realize the monitoring, analysis, and control of electromagnetic oscillation.

The wide-area measurement system (WAMS) is a dynamic real-time measurement and analysis platform for power systems, and it is widely used in system modeling, accident analysis, protection, and control [12]. The Phasor Measurement Unit (PMU) is a phasor measurement unit with the second pulse of Beidou or global positioning system as the synchronous clock [18], and it can provide basic data for the application analysis of WAMS. The traditional PMU mainly focuses on the line frequency signal in the range of 45~55 Hz, and it is usually necessary to filter out the interharmonic signal to improve the accuracy of phasor measurement [19]. Therefore, the traditional PMU cannot meet the multi-modal monitoring requirements of broadband electromagnetic oscillation. To address this problem, this paper proposes an adaptive band-pass filter and VMD-Esprit based multi-mode monitoring method of broadband electromagnetic oscillation in "double high" power systems for the multi-mode superposition characteristics of broadband oscillation. Firstly, wavelet filtering denoised the broadband signal and, through modal monitoring, obtained the initial modal information (frequency, amplitude, and initial phase). Then, the band is preliminarily decomposed according to the oscillation classification by the ABPF (adaptive band-pass filter) proposed in this paper. After the compensation link, VMD (Variational mode decomposition) further decomposes the preprocessing signal. Finally, the esprit modal parameter identification of each modal component obtained by VMD decomposition is carried out to obtain the desired signal information.

2. Methodology

After the description of the previous chapter, we have a preliminary understanding of the background of adaptive band-pass filter + VMD-Esprit based multi-Mode monitoring method of broadband electromagnetic oscillation in "double high" power systems, the overall framework of the method process and the innovation of this method. This chapter will focus on the application purpose, function, basic principles, and implementation process of each step in the process of this method. In addition, this chapter will emphatically expound on the design intention, implementation idea and application significance of the adaptive band-pass filter and VMD-Esprit signal identification algorithm are ed.

2.1. Adaptive Band-Pass Filter and VMD-Esprit Based Multi-Modal Monitoring Method

Through the analysis of the previous section, this section introduces the basic ideas and main steps of this research method in detail. This method takes the adaptive band-pass filter and VMD-Esprit as the core, combined with signal sampling, wavelet signal denoising and line frequency notch, to provide a new multi-mode electromagnetic oscillation monitoring and analysis method for wide area monitoring system and phasor monitoring device. In the following, the adaptive band-pass filter + VMD-Esprit based multi-modal monitoring method and its key technical methods are introduced in detail.

The basic idea of the method proposed in this paper is: (1) signal sampling and pre-processing. In the FFT modal monitoring link, according to the broadband oscillation classification using the adaptive band-pass filter proposed in this paper, decompose the broadband signal. (2) After compensation, the VMD is used to perform modal decomposition on each frequency band signal or directly perform the next identification. (3) The Esprit algorithm is used to perform identification on the decomposed modal information. The specific implementation process of this method is shown in Figure 1.

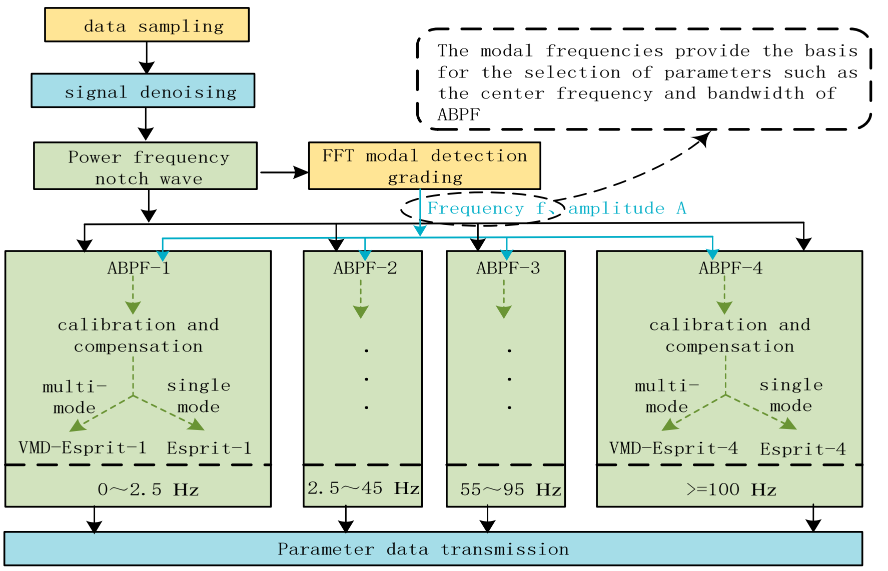

Note :
1. The maximum band-pass range of each ABPF is in the four bands of 1.0 ~ 2.5 Hz...
2. ABPF (Adaptive band-pass filter)
3. VMD (Variational mode decomposition)
4. Esprit (Estimation of signal parameters using rotational invariance tEchniques)

Figure 1. Flow chart of the broadband electromagnetic oscillation multi-mode monitoring method.

The following oscillation classification and signal transmission are based on the provisions of the "Technology specifications of power system wide-frequency measurement device" [20].

Step 1 data sampling. The node voltage and line current are sampled at a frequency of 10 kHz.

Step 2 signal denoising. Firstly, for subsequent signal processing, wavelet denoising is used to filter out noise and reduce external interference.

Step 3 line frequency notch. When the line oscillates, the line frequency signal is generally stable. In order to reduce the subsequent signal processing, the line frequency notch filter can quickly attenuate the line frequency and its nearby signals and has a superior filtering effect on the line frequency signal.

Step 4 modal monitoring. Based on Fast Fourier transform (FFT), the initial modal information (frequency f_0, amplitude A_0) is calculated, and the mode with amplitude A_{0i} ($i \leq n$ represents the ith mode, n represents the number of selected modes) that exceeds the set threshold A_{set} (where A_{set} can be set according to the actual operation of the l grid) is selected.

Step 5 oscillation classification filtering based on the adaptive band-pass filter (ABPF). According to the broadband oscillation classification, the center frequency, bandwidth, and other parameters of the band-pass filter are adaptively set for the case of multiple main frequency components in each frequency band, and the optimal frequency band separation is performed on the mode. If there is no strong signal in a certain frequency band (in the frequency band, there is no modal component that exceeds the threshold amplitude A_{set}), the band is not filtered.

Step 6 VMD-esprit. For each frequency band oscillation signal, adopt the VMD and adaptive band-pass filter to separate signals and then correct (the process of filtering will cause the signal's amplitude attenuation and the phase deviation). In the case that only one frequency component in a certain frequency band is obtained, the signal will be directly identified and separated in the previous step (adaptive band-pass filter, ABPF). In the case that two or more frequency components in the frequency band are obtained, VMD is used to decompose, and Esprit parameter identification is performed on the decomposed IMFs to obtain the desired signal parameters (amplitude, frequency, phase, and damping ratio).

Wavelet denoising is a relatively mature denoising algorithm. The specific algorithm implementation process and principle can be referred to in the references [21–23], and this article will not be repeated. The following explains the main technical methods of this method.

2.2. Key Technical Methods

2.2.1. Designations of Line Frequency Notch

The line frequency notch filter can quickly attenuate the signal near the line frequency and has an excellent filtering effect on the line frequency signal. The transfer function of the line frequency notch filter can be expressed as

$$G_{NF} = \frac{s^2 + (2\pi f_{NF})^2}{s^2 + 2\xi_{NF}(2\pi f_{NF})s + (2\pi f_{NF})^2} \tag{1}$$

In the equation, line frequency is f_{NF}, and notch factor is ξ_{NF}, respectively. Two factors of notch effect and dynamic are considered in the parameter design of the line frequency notch filter. The smaller the notch factor, the better the notch characteristics of the line frequency notch filter, but a smaller notch factor also leads to a decrease in frequency adaptability. According to Equation (1), when the notch factor is greater than 1.0, the characteristic equation has two unequal real poles on the negative real axis of the s-plane, which is in the overdamped state. When the notch factor is equal to 1.0, the characteristic equation has two equal real poles on the negative real axis of the s plane, which is in the critical damping condition. When Q is less than 1.0, the conjugate complex pole of the characteristic equation in the left half of the s plane is underdamped. Considering the notch characteristics and dynamic characteristics, the parameter design f_{NF} is 50 Hz, and the notch factor ζ_{NF} is set to 1.0.

2.2.2. Adaptive Band-Pass Filter (ABPF)

According to the "technical specifications for power system broadband measurement devices", the broadband oscillation in the new power system is divided into three parts, namely: low-frequency oscillation, sub/super synchronous oscillation, and 100~300 Hz broadband oscillation. The frequency range of various types of oscillations is different. Therefore, this paper designs four BPFs and proposes the concept of an adaptive band-pass filter (ABPF). Selecting the appropriate signal length can improve the accuracy of pattern recognition and ensure the rapidity of identification. Due to the different oscillation frequencies, it is obviously inappropriate to use data with the same duration and sampling frequency for identification. Table 1 shows these four ABPF filters' bandwidths, identification sampling times and sampling frequencies corresponding to various oscillations in this paper.

Table 1. Table showing the external parameter settings of ABPF for each frequency band.

Adaptive Band-Pass Filter	Oscillation Type	Sampling Time	Sampling Frequency	Oscillation Frequency Band
ABPF-1	Low-frequency oscillation	10 s	100	0~2.5 Hz
ABPF-2	subsynchronous oscillation	2 s	1000	2.5~45 Hz
ABPF-3	supersynchronous oscillation	2 s	1000	55~95 Hz
ABPF-4	wide-range-frequency oscillations	0.1 s	10,000	≥100 Hz

Through the analysis of the modal identification algorithm [24], if it is necessary to obtain the oscillation frequency and amplitude accurately, the sampling time of the identification signal needs to be more than one oscillation period. In order to obtain accurate damping ratio information, the sampling time needs to be higher than two oscillation cycles. Therefore, for low-frequency oscillation, in order to ensure the rapidity of identification, the minimum band-pass frequency of the band-pass filter is 0.2 Hz, and the sampling time is selected as two times the oscillation period, namely 10 s. For sub-synchronous oscillation, considering the comprehensive accuracy and identification speed, the minimum oscillation frequency is 2.5 Hz, and the sampling time is five times the oscillation period, namely 2 s. The mechanism of supersynchronous oscillation determines that it will appear in pairs with subsynchronous oscillation and that the frequency is complimentary. Therefore, the sampling time of supersynchronous oscillation is consistent with that of subsynchronous oscillation, which is also 2 s. The broadband oscillation is based on the lowest oscillation frequency of 100 Hz, and the sampling time is ten times the oscillation period, that is, 0.1 s.

The above four bands are only the maximum band-pass range of each band-pass filter. Considering that there are only one or more signals in each frequency band, the extraction of each frequency signal or the separation of frequency bands only through the filter with fixed parameters can easily lead to frequency aliasing or information redundancy in the frequency band. In order to avoid the above situation and pursue a better signal-filtering effect, this paper proposes the concept of ABPF. The design idea of ABPF in each frequency band is the same, taking any of them as an example, as shown in Figure 2.

f_{L} and f_{H} are the two frequency cut-off points of ABPF, and f_{C} is the center frequency. In this paper, digital filters are used, such as infinite impulse response (IIR) filters or finite impulse response (FIR) filters. The specific design method can be referred to in the references [25]. The ABPF expression used in this paper is as follows:

$$L_{BP}(z) = \frac{b}{2} \frac{\left(1+z^{-1}\right)\left(1-z^{-1}\right)}{1-(2+b-a^2)z^{-1}+(1+b)z^{-2}} \quad (2)$$

In the formula, a is the gain coefficient, b is related to the bandwidth, and the relationship between a and b is:

$$a = \frac{2\pi(1 - b/4)f_0}{f_s} \tag{3}$$

In the formula, f_s is the sampling frequency, and f_0 is the center frequency.

The adaptation of ABPF is reflected in two cases:

In Case 1, if there is only one signal in the frequency band, the band-pass filter is set to a narrowband band-pass filter, f_0 is the frequency of the signal, and the parameter b is set to a smaller value (the smaller the b is, the narrower the bandwidth is, which can be set according to the actual demand) to ensure the accuracy of this frequency signal filtering. In the next VMD decomposition of the filtered signal, it directly enters the Esprit parameter identification link. Only one signal does not need VMD decomposition because it itself is the desired modal component. This step of flexible design can reduce data processing time and data processing resources.

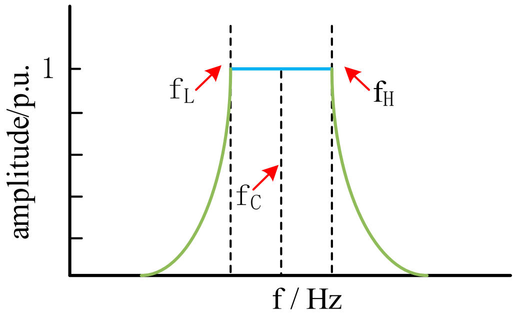

Figure 2. ABPF parameter design schematic.

In case 2, if there are multiple frequency signal components in the frequency band, the conventional band-pass filter center frequency is fixed. ABPF is adopted in this paper, and the first determined is not the center frequency but the cut-off frequencies f_L and f_H. The two parameters are determined by the two signals with the largest and smallest frequencies in the frequency band (with corresponding margins), adaptive setting of the center frequency (take the mean of the two), bandwidth, and other parameters. When there are multiple signals in the frequency band, the filter provides a more accurate signal decomposition for VMD, reducing the amount of calculation and improving the calculation speed.

This is the adaptive band-pass filter (ABPF) design method. These four ABPFs are cascaded using the same algorithm, as shown in Figure 3. The cascade processing of four ABPFs in different frequency bands can set the sampling time or sampling frequency according to the signal characteristics of different frequency bands to achieve the best signal processing effect. At the same time, it also reduces the number of decomposition modes of VMD. The segmented VMD decomposition greatly reduces the amount of calculation compared with the overall signal decomposition and improves the real-time performance and decomposition accuracy.

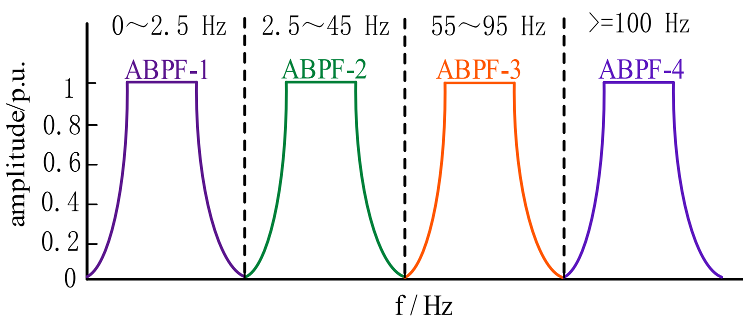

Figure 3. Four-band ABPF cascade.

2.2.3. Variational Mode Decomposition (VMD)

When dealing with nonlinear and non-stationary signals, VMD [26] is a new adaptive signal processing method with a strong anti-interference ability and strong robustness. VMD decomposition is a non-recursive signal decomposition algorithm. In different frequency bands, the signal is adaptively decomposed to the intrinsic mode functions (IMF). In the process of solving the modal function, the mirror extension avoids the end effect in the empirical mode decomposition (EMD) and other decomposition methods [27–30]. The processing of nonlinear fault signals by VMD is helpful in extracting the characteristics of subsequent fault signals. The decomposed IMF has an independent center frequency and sparsity and effectively avoids modal aliasing when the parameter values are appropriate.

For the broadband oscillation analysis of the new power system, phasor monitoring of time-varying and nonlinear oscillation signals should be carried out. To provide data support for the subsequent oscillation analysis, the accuracy and real-time performance should be taken into account during phasor monitoring. After the comparative demonstration, it is proposed to apply VMD to the broadband signal analysis of the new 'double high' power system. In this algorithm, VMD is used to decompose the multi-modal signal after ABPF filtering to prepare for the next parameter identification (Esprit). The VMD method will be introduced below.

VMD is a new type of non-stationary signal adaptive decomposition estimation method proposed by Konstantin Dragomiretskiy in 2014. The purpose is to decompose the original complex signal into K amplitude modulation sub-signals. EMD [31] and EEMD [32] use a recursive method to solve the mode, while the VMD method uses non-recursive and variational mode decomposition to process the original signal, which has better robustness to measurement noise. By setting reasonable convergence conditions, the number of modal functions decomposed by VMD is also smaller than that of EEMD, thus reducing the modeling complexity. VMD assumes that each 'mode' is a finite bandwidth with different center frequencies. The main process of this method is to use Wiener filtering to denoise. By initializing the finite bandwidth parameter a and the center angular frequency, K estimated center angular frequencies Wk are obtained. Then, the alternating direction multiplier method is used to update the modal function and its center frequency, and each mode is demodulated to the corresponding base frequency band. Finally, the purpose of minimizing the sum of estimated bandwidths of each mode is achieved.

VMD decomposition is widely used in various fields. Reference [33] applied VMD to decompose overvoltage signals. In Reference [34], VMD is applied to identify faults in the ring DC distribution network, and, using VMD, the author calculated the mutation energy of several modal components of voltage and current. Reference [35] applied VMD to detect and predict the failure of mechanical parts; in view of the multi-modal aliasing problem of current and voltage signals in the broadband electromagnetic oscillation analysis of power system, this paper decides to use VMD for modal decomposition after adaptive parameter filtering.

The VMD works as shown in Figure 4:

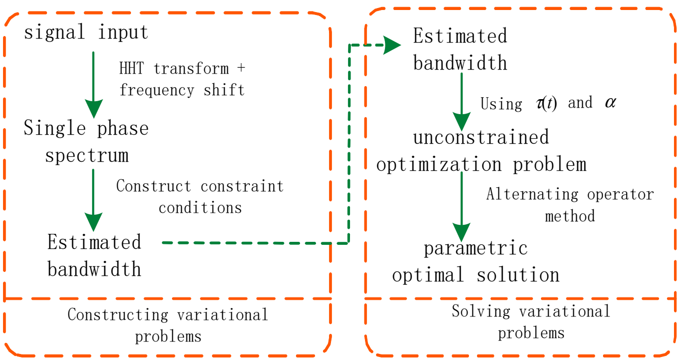

Figure 4. Variational mode decomposition of the VMD working principle.

Step 1 In order to obtain the one-way spectrum, the Hilbert transform is used to analyze and calculate each modal signal, and then the frequency shift method is used to move the modal spectrum to the baseband:

$$\left[\left(\delta(t)+\frac{j}{\pi t}\right)v_k(t)\right]e^{j\omega_k t} \tag{4}$$

$\delta(t)$ is the Dirac function; v_k and ω_k are the kth IMF component and its center frequency, respectively.

Step 2 The bandwidth is estimated by the square norm of the gradient. The constraint expression is:

$$\begin{cases} \min\limits_{\{v_k\},\{\omega_k\}}\left\{\sum\limits_{k=1}^{K}\|\partial_t\left[\left(\delta(t)+\frac{j}{\pi t}\right)v_k(t)\right]e^{-j\omega_k t}\|_2^2\right\} \\ s.t.\sum\limits_{k=1}^{K}v_k(t)=f(t) \end{cases} \tag{5}$$

where ∂_t is the gradient calculation and * is the convolution calculation symbol.

Step 3 In order to obtain the optimal solution more advantageously, the Lagrangian operator (t) and the penalty factor are used to transform the constrained problem into an unconstrained problem. The extended Lagrangian function expression is:

$$\mathrm{L}(\{v_k\},\{\omega_k\},\tau)=\alpha\sum_{k=1}^{K}\|\partial_t\left[\delta(t)+\frac{j}{\pi t}v_k(t)\right]e^{-j\omega_k t}\|_2^2+\|f(t)-\sum_{k=1}^{K}v_k(t)\|_2^2+\left[\tau(t),f(t)-\sum_{k=1}^{K}v_k(t)\right] \tag{6}$$

Step 4 The alternating direction method of multipliers is used to iteratively update the modal components and the center frequency, and the saddle point of the unconstrained function is obtained, which is the optimal solution to the problem. The iterative update expressions of v_k and k are as follows:

$$\hat{v}_k^{n+1}(\omega)=\frac{\hat{f}(\omega)-\sum\limits_{i\neq k}\hat{v}_i(\omega)+\frac{\hat{\tau}(\omega)}{2}}{1+2\alpha(\omega-\omega_k)^2} \tag{7}$$

$$\omega_k^{n+1}=\frac{\int_0^\infty \omega|\hat{v}_k(\omega)|^2 d\omega}{\int_0^\infty |\hat{v}_k(\omega)|^2 d\omega} \tag{8}$$

$$\hat{\tau}^{n+1}(\omega)=\hat{\tau}^n(\omega)+\gamma\left[\hat{f}(\omega)-\sum_{k=1}^{K}\hat{u}_k^{n+1}(\omega)\right] \tag{9}$$

Equation (9) n is the number of iterations, and γ is the noise margin parameter.

Step 5 The iteration termination condition is determined. If Equation (7) holds, the iteration is stopped, and the modal component is output.

$$\frac{\sum\limits_{k=1}^{K}\|\hat{v}_k^{n+1}-\hat{v}_k^n\|_2^2}{\sum\limits_{k=1}^{K}\|\hat{v}_k^n\|_2^2}<\varepsilon \tag{10}$$

VMD has certain limitations in processing signals. In addition, the algorithm needs to first set the modal number K value, which is the number of IMF components. When K is selected properly, the frequency components in the original signal can be well decomposed. Improper values will cause under-decomposition or over-decomposition. The α value affects the bandwidth of the IMF. A bandwidth that is too small will cause some signals to be decomposed and to be lost. Otherwise, if the bandwidth is too long, the decomposition signals will mix with other components. Therefore, the selection of α and K will affect the decomposition effect of the VMD method.

Of course, for the parameter selection problem, there are some mature methods to determine the best parameters. In Reference [36], the sparrow algorithm search algorithm (SSA) will optimize the decomposition mode number K and penalty factor α for the VMD algorithm. In [37], the energy factor and information entropy are introduced as constraints to adaptively determine the number of modal decompositions and penalty factors. Reference [38] proposed a parameter alternating optimization method to optimize the parameters of VMD. Reference [39] determined the number of decompositions based on the correlation coefficient of each component and used particle swarm optimization to optimize the penalty factor. In this paper, only the basic VMD decomposition method is used to provide an idea of applying VMD to broadband analysis. The optimization of related improved algorithms will be optimized in subsequent articles.

2.2.4. Esprit Parameter Identification

Esprit (Estimation of Signal Parameters using Rotational Invariance Techniques) is a high-resolution algorithm for estimating signal parameters by the number of rotation invariant sets. Although it has no application in the analysis of broadband signals in power systems combined with VMD or filter signals, it has applications in other fields, such as the application of TLS-Esprit for flicker detection in ref. [40]. Ref. [41] applied TLS-Esprit to construct a time-frequency curve and signal envelope of rotor broken bar fault detection methods, and the TLS-Esprit algorithm in ref. [42] extracts the frequency of the dominant component in the electrical fluctuation and calculates the phase parameters. In view of the fact that Esprit can extract waveform parameter information, this paper proposes to combine Esprit and VMD decomposition, namely the VMD-Esprit algorithm, and also uses Esprit to identify the parameters of the signal filtered by the adaptive band-pass filter. The algorithm provides a new idea for modal parameter identification of broadband electronic oscillation in power systems.

Esprit is not sensitive to noise and does not need to search for spectral peaks in the whole time domain. It is widely used in the field of signal processing. Compared with Prony, Hilbert, and other parameter identification algorithms, it has the advantages of low computational complexity and low parameter requirements. Through the comparison and demonstration of this algorithm, this Esprit algorithm is combined with VMD for parameter identification.

The basic principle of the Esprit algorithm [43] is as follows. The Hankel matrix X is constructed according to the preprocessed measured data sequence $x_0, x_1, \ldots, x_{N-1}$, as shown in Equation (11) [44]:

$$X = \begin{bmatrix} x_0, x_1, \ldots, x_{M-1} \\ x_1, x_2, \ldots, x_M \\ \ldots. \\ x_{L-1}, x_L \ldots., x_{N-1} \end{bmatrix} \tag{11}$$

Among them, M + L − 1 = N, the signal subspace vs. and noise subspace V_n are obtained by singular value decomposition of X:

$$X(SVD) = U\sum V^H = [U_s, U_n] \begin{bmatrix} \varepsilon_s & 0 \\ 0 & \varepsilon_s \end{bmatrix} \begin{bmatrix} V_s^H \\ V_n^H \end{bmatrix} \tag{12}$$

The superscript H represents the conjugate transpose, $\sum$ is the diagonal matrix, the diagonal elements are the singular values of the matrix X in descending order, the column vector of V is the right eigenvector of the matrix X, and the column vector of vs. corresponds to the eigenvectors of the P singular values with the largest amplitude of the matrix X. The first row and the last row of vs. are deleted to obtain the reduced-dimensional signal subspace V_1, V_2. There exists a unique invertible transformation matrix T such that

$V_1 = V_{2T}$. Let U be the original signal. Similarly, the original signal subspace U_1, U_2 are obtained, which satisfies:

$$\begin{aligned} U_1 &= V_1 T \\ U_2 &= V_2 T \\ U_2 &= U_1 \psi \end{aligned} \tag{13}$$

U_1 and U_2 are known quantities obtained by data matrix decomposition, so the matrix shown in Equation (14) can be constructed to estimate the signal.

$$\psi = \left(U_1^H U_1\right)^{-1}\left(U_2^H U_2\right) \tag{14}$$

If the eigenvalue of Ψ is λ_p, the frequency ω_p and attenuation coefficient ω_p of each periodic component in the signal can be estimated according to Equation (15).

$$\begin{aligned} \omega_p &= \frac{\arg\lambda_p}{T_s} \\ \sigma_p &= -\frac{\ln\left|\lambda_p\right|}{T_s} \end{aligned} \tag{15}$$

After obtaining the frequency and attenuation coefficient of each component in the signal, the amplitude and initial phase information can be obtained by the least square method. Assuming an N-point sampling signal, the least square method is used to obtain:

$$c = (c_1, c_2, \ldots, c_p) = \left(\lambda^H \lambda\right)^{-1} \lambda^H Y \tag{16}$$

$$\lambda = \begin{bmatrix} 1, & 1, & \ldots & 1 \\ \lambda_1, & \lambda_2 & & \lambda_p \\ & & \ldots & \\ \lambda_1^{N-1}, & \lambda_2^{N-1} & \ldots & \lambda_p^{N-1} \end{bmatrix} \tag{17}$$

The amplitude and phase are:

$$\begin{aligned} \alpha_p &= 2\left|c_p\right| \\ \varphi_p &= \arg \mathrm{c}_p \end{aligned} \tag{18}$$

Like the VMD algorithm, Esprit also has a corresponding improved algorithm. The more classic algorithm is TLS-Esprit [45]; ref. [46] introduced the algorithm. In addition, the related optimization algorithm is the MSWF-ESPRIT algorithm. Ref. [47] pointed out that the combination of its principle and multi-dimensional filter can effectively reduce the total least squares rotation invariant subspace algorithm to estimate the covariance matrix of the display data and the eigenvalue decomposition of the high-order matrix. This paper uses the rotation invariant technique based on a multi-dimensional filter to estimate the signal parameter method to estimate the frequency of the interharmonic signal. In this paper, the most basic Esprit algorithm is used to provide a new idea of combining Esprit with VMD/filter in the new power system broadband electromagnetic oscillation problem. The application of the improved algorithm in the power system broadband oscillation problem will be further studied.

3. Results

3.1. Validation and Analysis Based on the Construct Signal

The constructed signal decomposed in this paper is shown in Equation (19) below.

$$\begin{aligned} x(t) = \quad & A_1\cos(2\pi f_1 t + \varphi_1) + A_2\cos(2\pi f_2 t + \varphi_2) + A_3\cos(2\pi f_3 t + \varphi_3) + A_4\cos(2\pi f_4 t + \varphi_4) + \\ & A_5\cos(2\pi f_5 t + \varphi_5) + A_6 random[-1,\ 1] \end{aligned} \tag{19}$$

In the formula: A_1 = 5 V; A_2 = 5 V; A_3 = 5 V; A_4 = 5 V; A_5 = 5 V; A_6 = 0.16; f_1 = 1.5; f_2 = 25; f_3 = 50; f_4 = 300; f_5 = 400; $\varphi_1 = \Pi/3$; $\varphi_2 = \Pi/4$; $\varphi_3 = \Pi/2$; $\varphi_4 = \Pi/3$; $\varphi_5 = \Pi/3$.

In order to test the notch performance of the line frequency notch filter, the denoising effect of wavelet denoising, the adaptive performance of the adaptive band-pass filter ABPF, the decomposition effect of VMD decomposition, and the accuracy of parameter identification, this paper constructs a signal composed of a low-frequency constant amplitude oscillation signal, a subsynchronous constant amplitude oscillation signal, two broadband constant amplitude oscillation signals, and the line frequency (50 Hz)and noise signal.

As shown in Figure 5, after the line frequency notch, the waveform is basically consistent with the signal waveform without line frequency, which proves that the performance of the common frequency notch is excellent. As shown in Figure 6a, when the original signal contains noise, modal decomposition and other links will be greatly influenced. After wavelet denoising, the signal waveform of noise removal shown in Figure 6b basically coincides with the waveform without noise, which proves the practicability and relatively good performance of wavelet denoising in the broadband field.

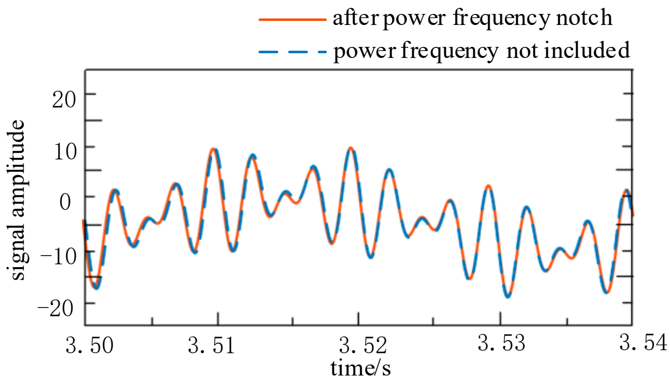

Figure 5. Comparison of the signal after the line frequency notch and the signal without the line frequency notch.

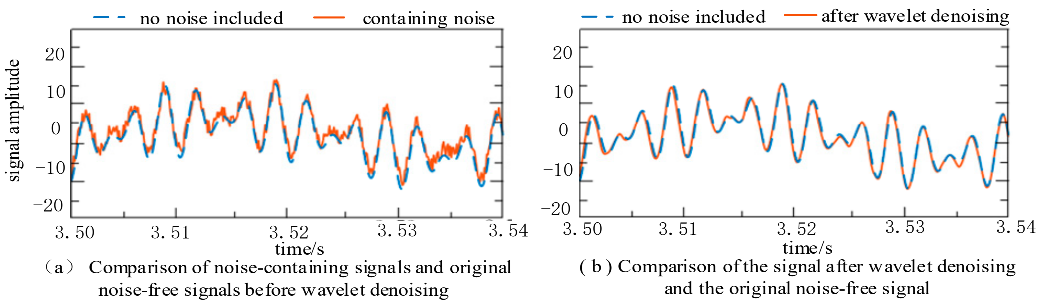

Figure 6. Comparison of each signal before and after wavelet denoising.

After FFT modal detection grading and classification, the sub-band ABPF filtering is performed, and then the phase compensation is performed. As shown in Figure 7, the phase compensation waveform is compared before and after because the ABPF filtering causes the extracted signal component amplitude or phase to deviate from the original signal, so the filtered waveform needs to be compensated in order to make the subsequent parameter identification more accurate. From the diagram, the compensation result can be seen that after this link, the compensated waveform coincides with the original waveform. This link achieves the desired effect.

By comparing the ABPF filtering waveforms of 1.5 Hz and 25 Hz shown in Figure 8 with the original waveforms, it can be seen that after a period of filtering, the obtained waveform is compensated and coincides with the original waveform. The use of filters effectively avoids the problems of large calculations and difficult parameter selection for each signal decomposition algorithm. At the same time, the filter separates the components of the original signal, which also avoids the problem of error or synchronization and poor real-time performance when Esprit parameter identification or waveform reconstruction is performed after VMD decomposition.

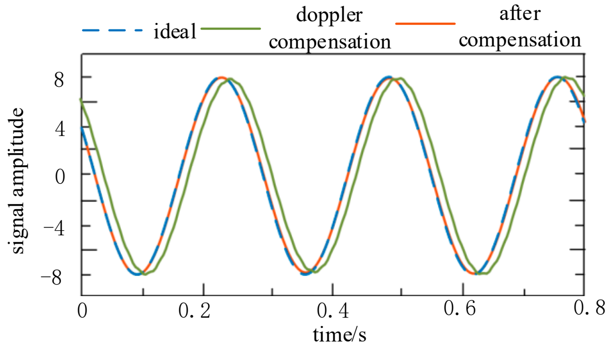

Figure 7. Comparison of phase compensation waveform before and after.

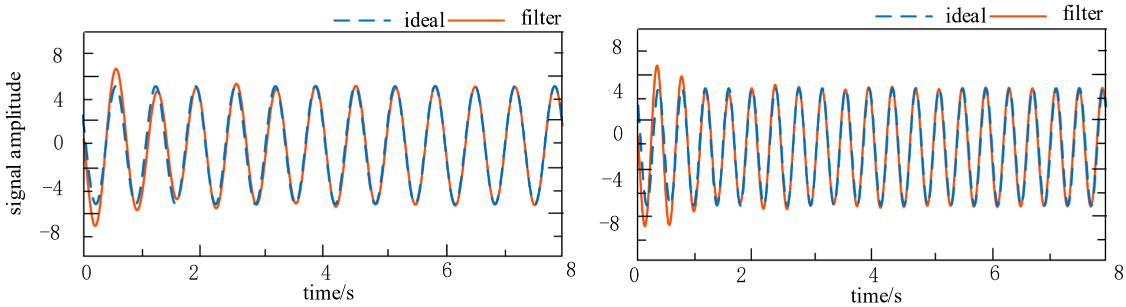

(a) Comparison of 1.5 Hz filtered waveform and original signal waveform

(b) 25 Hz filter waveform and the original signal waveform comparison chart

Figure 8. Comparison of 1.5 Hz, 25 Hz filter waveform with the original signal waveform.

As shown in Figure 9, the waveform of the two main frequencies (300 and 400 Hz) in the high-frequency band after ABPF filtering is compared with the waveform of the original two frequencies. It can be seen that the two waveform curves coincide, and the filtering effect is very good. Figure 10a,b is the comparison between the 300 and 400 Hz modal components obtained by VMD decomposition of the original filtered and compensated waveform and the original ideal waveform. It can be seen that the effect of modal decomposition is very good. The waveform drawn by the two modes coincides with the waveform filtered by the filter. It is also seen that VMD decomposition is suitable for high-frequency bands and overcomes the spectrum aliasing problem in filter filtering.

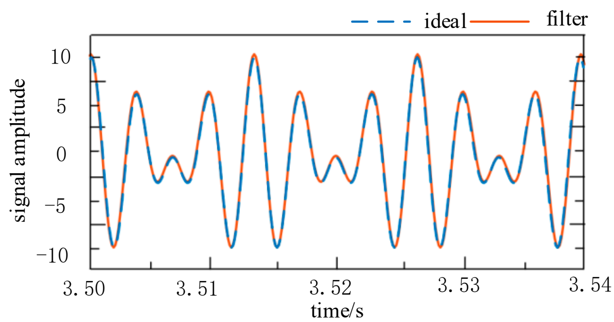

Figure 9. 300 Hz + 400 Hz undecomposed filter waveform and the original signal waveform comparison.

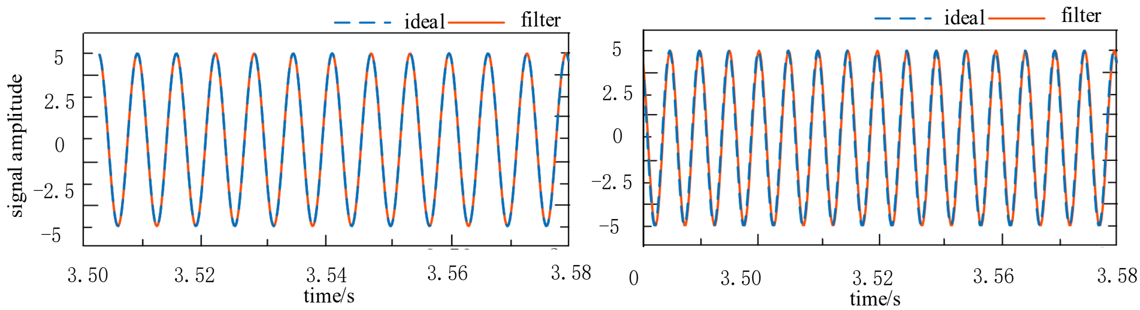

(a) VMD decomposition mode 1 (300Hz) waveform compared with the original waveform

(b) Comparison of VMD decomposition mode 2 (400Hz) waveform with the original waveform

Figure 10. 300, 400 Hz VMD mode decomposition waveform and their original signal waveform comparison chart.

The modal parameters are calculated by Esprit, the theoretical value and parameter identification results are compared, and the relative error is calculated as shown in Table 2 below. The frequency identification result is the best, and the amplitude and phase angle identification also meet the engineering requirements. The deviation of the phase angle identification result is slightly larger, and the subsequent phase angle parameter identification algorithm needs to be further improved.

Table 2. Precision test results of each parameter.

Adaptive Band-Pass Filter	Parameter	Theoretical Value	Identification Value	Relative Error/%
Mode 1	amplitude	5 V	4.9344 V	1.312
	frequency	1.5 Hz	1.5000 Hz	0.000
	phase angle	Π/3	1.0524	0.506
Mode 2	amplitude	5 V	4.9006 V	1.988
	frequency	25 Hz	25.0000 Hz	0.000
	phase angle	Π/4	0.7283	7.277
Mode 3	amplitude	5 V	4.8862 V	2.228
	frequency	300 Hz	300.0000 Hz	0.000
	phase angle	Π/3	0.9587	8.442
Mode 4	amplitude	5 V	4.8862 V	2.228
	frequency	400 Hz	400.0000 Hz	0.000
	phase angle	Π/3	0.9059	13.484

Through the application of the algorithm proposed in this paper in the above-mentioned example, the waveform effect obtained by the ABPF with the compensation algorithm is very good, and the deviation between the modal components obtained by the application of the VMD-Esprit algorithm and the original waveform is also small, and the parameter identification effect is good. These characteristics meet the engineering application requirements. The feasibility of the method proposed in this paper is preliminarily demonstrated.

3.2. Broadband Osillation in Weak Grid with Two VSCs

As shown in Figure 11, the two VSCs are interconnected into the weak grid, and one of the stations has an oscillation spreading to the main grid. The parameters of the system in the example are as follows:

$$R_{12} = 0.001\ \Omega,\ R_{13} = 0.001\ \Omega,\ R_{14} = 0.001\ \Omega,\ L_{12} = 0.00029\ \text{H},\ L_{12} = 0.00029\ \text{H},\ L_{14} = 0.00001\ \text{H}.$$

The proposed adaptive band-pass filter and VMD-Esprit based multi-mode monitoring method of broadband electromagnetic oscillation in "double high" power systems is used to decompose the oscillation, and the accuracy of the decomposition results is verified. After sampling the digital-to-analog conversion, wavelet denoising and line frequency notch, the initial i_{12a} is subjected to FFT analysis in the modal detection link. The spectrum is shown in Figure 12:

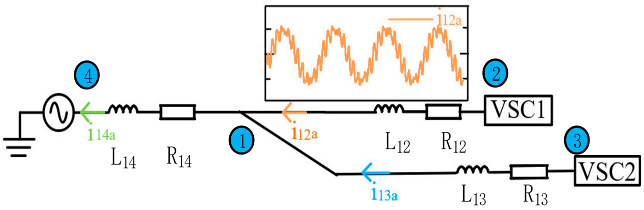

Figure 11. Example space diagram and resonant branch waveform.

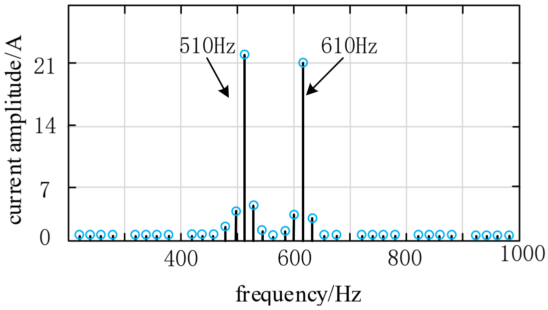

Figure 12. FFT spectrum diagram of the modal detection link.

By setting the threshold and Filtering processing of ABPF (this oscillation signal only has a broadband oscillation component), there are two components that continue to perform VMD decomposition. In order to verify the accuracy of separating the two components, the second-order band-pass filter is used to extract the two signal components from the original signal, and the filtered signal component and the VMD two-mode component are drawn into a graph, as shown in Figure 13a is the comparison graph corresponding to 510 Hz, and Figure 13b is the comparison graph corresponding to 610 Hz. It can be seen that the results of VMD modal decomposition coincide with the curves of each modal component processed by the filter, which proves the accuracy and engineering application of VMD decomposition.

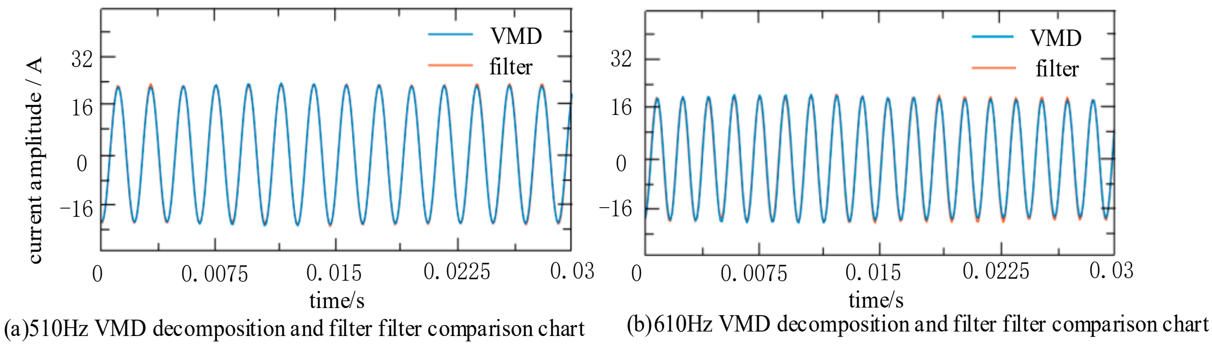

Figure 13. VMD modal decomposition of each modal waveform and filter waveform comparison.

4. Discussion

In this paper, an adaptive band-pass filter and VMD-Esprit based multi-Mode monitoring method of broadband electromagnetic oscillation in "double high" power systems is proposed, which overcomes the limitations of traditional monitoring methods for electromagnetic resonance monitoring. It provides a new idea for broadband signal decomposition and broadband oscillation analysis. The algorithm also takes into account both measurement accuracy and operation speed.

The line frequency notch link is aimed at the line frequency of 50 Hz and remains stable when broadband oscillation occurs in the power system. Compared with the literature [48–50], although different methods are used to decompose the signal of the power system and identify the parameters, the authors of the three publications consider the decomposition and identification of the line frequency 50 Hz signal. On the one hand, this method reduces the influence of line frequency amplitude and frequency on the analysis of broadband oscillation signals and focuses on the analysis of broadband oscillation signals. On the other hand, filtering the line frequency signal can also reduce the amount of calculation in the subsequent steps.

There are many kinds of noise in the imaging system, such as thermal noise caused by resistance; shot noise and flicker noise caused by vacuum devices; the particle noise generated by the surface junction transistor; and so on [51], and for the huge power system with the wide application of millisecond power electronic devices, the influence of noise on the waveform processing can not be ignored. The original intention of wavelet denoising is also because of this. Wavelet denoising is used to reduce the interference of noise on subsequent signal analysis. The signal preprocessing through these two links provides a better signal for subsequent modal detection, adaptive band-pass filtering and signal decomposition and identification.

The FFT modal detection grading link [51,52] initially identifies the frequency and amplitude information of the resonant mode. It provides a basic data reference for subsequent band-pass filters and also provides a basis for setting signal processing thresholds.

According to the "Technical Specification for Power System Broadband Measurement Devices" [20], the ABPF (adaptive band-pass filter) designed in this paper is used to perform parallel data processing of broadband electromagnetic oscillation signals in different frequency bands, which reduces the signal processing order (VMD decomposition mode number) while improving the efficiency and accuracy of signal decomposition and real-time performance. The problem of high order and poor real-time performance of the overall signal directly using VMD decomposition is avoided. According to the signal characteristics of different frequency bands, the sampling time or sampling frequency is set [53], and the best signal processing effect can be achieved by targeted sampling according to the oscillation signals of different frequency bands.

The ABPF is realized by a digital filter, which avoids the complexity of analog filter design [54,55] and improves the effectiveness and accuracy of signal decomposition. At the same time, the application of digital filters can directly set the band-pass width, attenuation gain, and other parameters. In order to increase the filtering flexibility, some parameters can also be set independently for user needs. For the ABPF, the adaptive parameter method of the band-pass filter proposed in this paper enables the band-pass filter to adaptively adjust the center frequency, bandwidth, and other parameters when processing the signals in the frequency band under different conditions of single-mode composite or multi-mode composite. In this way, the signal can be directly extracted and entered into the parameter identification link when the single mode is composed, which avoids the next signal decomposition process of the fixed parameter filter in any case, reduces the calculation amount, and makes the algorithm process more flexible. It can also provide more accurate decomposition signals for VMD in the case of multi-signal synthesis and improve the calculation speed.

When VMD is applied to the analysis of broadband electromagnetic oscillation signals, the algorithm overcomes the shortcomings of traditional EMD, EEMD, and other modal decomposition algorithms, such as fence effect, modal aliasing, and low mathematical basis. At the same time, the Esprit parameter identification algorithm for fault identification and radar and other fields is combined with VMD to overcome the defects of traditional VMD modal parameter identification algorithms (Prony or HT, etc.), such as parameter selection, noise sensitivity, and inaccurate identification of high-frequency signals, which is groundbreaking.

In summary, this paper provides a new idea for signal decomposition and parameter identification in broadband measurement devices through the initial signal preprocessing links (line frequency notch, wavelet denoising, FFT modal detection grading) and then through combining the proposed ABPF (adaptive band-pass filtering) with VMD-Esprit achieve multi-Mode monitoring method.

Author Contributions: Conceptualization, C.L. and H.Y.; methodology, C.S.; software, J.C.; validation, H.Y. and C.S.; formal analysis, T.Z.; investigation, J.C.; resources, C.L.; data curation, C.S.; writing—original draft preparation, H.Y.; writing—review and editing, C.S. All authors have read and agreed to the published version of the manuscript.

Funding: This research received no external funding.

Data Availability Statement: The data presented in this study are available on request from the corresponding author.

Conflicts of Interest: The authors declare no conflict of interest.

References

1. Bai, J.; Xin, S.; Liu, J.; Zheng, K. Roadmap of realizing the high penetration renewable energy in China. *Proc. CSEE* **2015**, *35*, 3699–3705.
2. Zhou, X.; Chen, S.; Lu, Z.; Huang, Y.; Ma, S.; Zhao, Q. Technology features of the new generation power system in China. *Proc. CSEE* **2018**, *38*, 1893–1904.
3. Peng, L.; Chen, G.; Dong, C. Development of technologies in ±1500 kV UHV DC transmission research. *High Volt. Eng.* **2017**, *43*, 3137–3148.
4. Liang, X.; Zhang, P.; Chang, Y. Recent Advances in High-Voltage Direct-Current Power Transmission and Its Developing Potential. *Power Syst. Technol.* **2012**, *36*, 1–9. [CrossRef]
5. Zhang, W.-L.; Yu, Y.-Q.; Li, G.-F.; Fan, J.-B.; Su, Z.-Y.; Lu, J.-Y.; Li, B. Researches on UHVDC Technology. *Proc. CSEE* **2007**, *27*, 1–7.
6. Tang, W.; Zhang, Q.; Zhang, L.; Zhang, B.; Zhang, Y. Concept, Key Technoligies and Development Direction of Multilevel AC/DC Interconnection in New Distribution System [J/OL]. *Autom. Electr. Power Syst.* **2023**, 1–16. Available online: http://kns.cnki.net/kcms/detail/32.1180.TP.20230217.1019.002.html (accessed on 28 February 2023).
7. Teodorescu, R.; Liserre, M.; Rodriguez, P. *Grid Converters for Photovoltaic and Wind Power Systems*; John Wiley & Sons: Hoboken, NJ, USA, 2011.
8. Wang, X.; Blaabjerg, F.; Wu, W. Modeling and analysis of harmonic stability in an AC powerelectronics-based power system. *IEEE Trans. Power Electron.* **2014**, *29*, 6421–6432. [CrossRef]
9. Ma, N.; Xie, X.; He, J.; Wang, H. Review of Wide-band Oscillation in Renewable and Power Electronics Highly Integrated Power Systems. *Proc. CSEE* **2020**, *40*, 4720–4732. [CrossRef]
10. Chen, L.; Xu, S.; Sun, H.; Bi, J.; Song, R.; Yi, J.; Guo, Q. A Survey on Wide-frequency Oscillation for Power Systems with High Penetration of Power Electronics. *Proc. CSEE* **2021**, *41*, 2297–2310. [CrossRef]
11. Xie, X.; Liu, H.; He, J.; Liu, H.; Liu, W. On New Oscillation Issues of Power Systems. *Proc. CSEE* **2018**, *38*, 2821–2828+3133. [CrossRef]
12. Wang, L.; Xie, X.; Jiang, Q.; Liu, H.; Li, Y.; Liu, H. Investigation of SSR in practical DFIG-based wind farms connected to a series-compensated power system. *IEEE Trans. Power Syst.* **2015**, *30*, 2772–2779. [CrossRef]
13. Xie, X.; Zhang, X.; Liu, H.; Liu, H.; Li, Y.; Zhang, C. Characteristic analysis of subsynchronous resonance in practical wind farms connected to series-compensated transmissions. *IEEE Trans. Energy Convers.* **2017**, *32*, 1117–1126. [CrossRef]
14. Liu, H.; Xie, X.; He, J.; Xu, T.; Yu, Z.; Wang, C.; Zhang, C. Subsynchronous interaction between direct-drive PMSG based wind farms and weak AC networks. *IEEE Trans. Power Syst.* **2017**, *32*, 4708–4720. [CrossRef]
15. Liu, H.; Xie, X.; Liu, W. An oscillatory stability criterion based on the unified dq-frame impedance network model for power systems with high-penetration renewables. *IEEE Trans. Power Syst.* **2018**, *33*, 3472–3485. [CrossRef]
16. Adams, J.; Carter, C.; Huang, S.H. ERCOT experience with sub-synchronous control interaction and proposed remediation. In Proceedings of the 2012 IEEE PES Transmission and Distribution Conference and Exposition, Orlando, FL, USA, 7–10 May 2012; IEEE: Piscataway, NJ, USA, 2012; pp. 1–5.
17. Buchhagen, C.; Rauscher, C.; Menze, A.; Jung, J. BorWin1—First experiences with harmonic interactions in converter dominated grids. In Proceedings of the International ETG Congress 2015, Die Energiewende—Blueprints for the New Energy Age, Bonn, Germany, 17–18 November 2015; VDE: Frankfurt am Main, Germany, 2015; pp. 1–7.
18. Maheswari, M.; Vanitha, N.S.; Loganathan, N. *Wide-Area Measurement Systems and Phasor Measurement Units*; Springer: Cham, Switzerland, 2020; pp. 105–126.
19. Xu, S.; Liu, H.; Bi, T. Reference value measurement algorithms for PMU field test and calibration. *Proc. CSEE* **2020**, *40*, 3452–3461. (In Chinese)

20. *GDW12214-2022*; State Grid Corporation of China. Technology Specifications of Power System Wide-Frequency Measurement Device. Electric Power Press: Beijing, China, 2022.
21. Fan, X.-L.; Xie, W.-C.; Jiang, W.-B.; Li, Y.; Huang, X.-L. An Improved Threshold Function Method for Power Quality Disturbance Signal De-Noising Based on Stationary Wavelet Transform. *Trans. China Electrotech. Soc.* **2016**, *31*, 219–226. [CrossRef]
22. Sun, S.-G.; Pang, Y.; Wang, J.-Q.; Zhang, C.; Du, T.-H.; Yu, H. EEMD harmonic detection method based on the new wavelet threshold denoising pretreatment. *Power Syst. Prot. Control* **2016**, *44*, 42–48.
23. Dai, D.-D.; Wang, X.-P.; Long, J.-C.; Tian, M.; Zhu, G.-W.; Zhao, L. De-Noising Method of Ultra-high Frequency Partial Discharge Signal Based on Improved Protrugram and Wavelet Transform. *High Volt. Eng.* **2018**, *44*, 3577–3586. [CrossRef]
24. HAUER, J.F.; DEMEURE, C.J.; SCHARF, L.L. Initial results in Prony analysis of power system response signals. *IEEE Trans. Power Syst.* **1990**, *5*, 80–89. [CrossRef]
25. Zhao, Y.; Du, H.; Zhang, Z. The Application of MATLAB in the Design and Sim ulation of one kind IIR Digital Dandpass Filter. *Microcomput. Inf.* **2007**, *200*, 285–287+233.
26. Dragomiretskiy, K.; Zosso, D. Variational Mode Decomposition. *IEEE Trans. Signal Process.* **2014**, *62*, 531–544. [CrossRef]
27. Rilling, G.; Flandrin, P.; Gonçalvès, P. On empirical mode decomposition and its algorithms. In Proceedings of the IEEE-EURASIP Workshop Nonlinear Signal Image Process (NSIP), Trieste, Italy, 8–11 June 2003; Volume 3, pp. 8–11.
28. Sharpley, R.C.; Vatchev, V. Analysis of the intrinsic mode functions. *Construct. Approx.* **2005**, *24*, 17–47. [CrossRef]
29. Rilling, G.; Flandrin, P. One or two frequencies? The empirical mode decomposition answers. *IEEE Trans. Signal Process.* **2008**, *56*, 85–95. [CrossRef]
30. Rilling, G.; Flandrin, P. Sampling effects on the empirical mode decomposition. *Adv. Adapt. Data Anal.* **2009**, *1*, 43–59. [CrossRef]
31. Xu, X.-G.; Xu, G.-L.; Wang, X.-T.; Qin, X.-J. Empirical Mode Decomposition and its Application. *Acta Electron. Sin.* **2009**, *37*, 581–585.
32. Zheng, J.-D.; Cheng, J.-S.; Yang, Y. Modified EEMD algorithm and its applications. *J. Vib. Shock.* **2013**, *32*, 21–26+46. [CrossRef]
33. Yang, D.; Chen, S.; Liu, X.; Gao, L.; Wang, Y. Research on Overvoltage Signal Recognition Based on Adaptive VMD and Time-frequency Segment Energy Entropy. *Power Syst. Technol.* **2019**, *43*, 4597–4604. [CrossRef]
34. Gao, S.; Lyu, Y.; Song, G.; Shen, Q.; Li, Y. DC Distribution Network Protection Method Using Improved VMD Sudden Change Energy. *J. Xian Jiaotong Univ.* **2022**, 1–11. Available online: http://kns.cnki.net/kcms/detail/61.1069.t.20221213.1740.003.html (accessed on 2 March 2023).
35. Zhou, C.; Xu, M.; Jia, Y.; Ye, Z.; Yang, P.; Yuan, X. Adaptive VMD and its application in state tracking and fault detection. *J. Electron. Meas. Instrum.* **2022**, 1–13. Available online: http://kns.cnki.net/kcms/detail/11.2488.TN.20221215.1152.005.html (accessed on 2 March 2023).
36. Yu, H.; Lin, T.; Qi, M. Fire-storage combined frequency regulation strategy based on SSA-VMD and double-layer fuzzy control. *J. Power Supply* **2022**, 1–15. Available online: http://kns.cnki.net/kcms/detail/12.1420.TM.20221202.1543.003.html (accessed on 2 March 2023).
37. Li, S. Single Channel Blind Source Separation based on Improved VMD Rolling Bearing Composite Fault Diagnosis. Master's Thesis, Harbin University of Science and Technology, Harbin, China, 2021. [CrossRef]
38. Song, X.; Gao, Y.; Ding, G.; Li, T. Study on transmission line traveling wave fault location based on improved VMD participation. *Electrotech. Appl.* **2019**, *38*, 26–33.
39. Zheng, X.; Chen, G.; Ren, H.; Li, D. Fault detection of vulnerable units of wind turbine based on improved VMD and DBN. *J. Vib. Shock.* **2019**, *38*, 153–160+179. [CrossRef]
40. Zhang, J.-J.; Yang, H.-G. Application of TLS-ESPRIT in estimation of voltage flicker. *Power Syst. Prot. Control.* **2009**, *37*, 44–48.
41. Gao, L.-Q. Reasearch on Roter Broken Bar Fault Detection of Induction Moter under Variable Frequency Speed Regulation. Master's Thesis, China University of Mining and Technology, Beijing, China, 2022. [CrossRef]
42. Zheng, B.; Feng, S.; Wu, X. Detection of Forced Oscillations Source Based on WAMS. *Jiangsu Electr. Eng.* **2016**, *35*, 32–34+43. [CrossRef]
43. Yang, H.; Lv, W.; Guan, Y.; Chen, X.; Wu, X. Power oscillation detection method based on higher order cumulant and ESPRIT algorithm. *Electr. Meas. Instrum.* **2021**, *58*, 37–45. [CrossRef]
44. Long, J.-T.; Wang, Q.-F.; Liao, F.-F. Identification of Power System Low Frequency Oscillation Mode Based on Fourth-order Mixed Mean Cumulant and TLS-ESPRIT Algorithm. *Smart Power* **2019**, *47*, 67–72.
45. Zhang, J.-J.; Yang, H.-G. TLS-ESPRIT for Interharmonic Estimation. *Proc. CSU-EPSA* **2010**, *22*, 70–75.
46. Yan, H.; Hu, Y.; Tai, N.-L. An Improced Relay Protection Algotithm Suitable for Wind Farm Connecting Transmission Line. *Water Resour. Power* **2016**, *34*, 209–212.
47. Luo, R.-C.; Huang, B.; Yang, Y.-Z. Inter-harmonics Parameter Analysis via Double Population PSO and MSWF-ESPRIT. *Proc. CSU-EPSA* **2014**, *26*, 12–16+33.
48. Geng, Z.-X.; Zhang, F.-S. The Calibrating Method of Total Harmonic Components of Power System. *Proc. CSEE* **2018**, *38*, 3481–3487+7. [CrossRef]
49. Dou, J.-W.; Yang, X.-Y.; Yang, X.-Z. A Power System Harmonic Detection Method Based on Fractional Wavelet Transform. *Proc. CSEE* **2022**, 1–9. [CrossRef]
50. Qiu, W.; Tang, Q.; Tang, L.; Li, J.-M.; He, J. Power System Harmonic Analysis Under Non-stationary Situations Based on Quasi-synchronous and Sequence Reconstruction. *Proc. CSEE* **2018**, *38*, 456–464+676. [CrossRef]

51. Liu, G.-H.; Guo, W.-M. Application of improved arithmetic of median filtering denoising. *Comput. Eng. Appl.* **2010**, *46*, 187–189.
52. Chen, Z.-T.; Xu, J.; Li, G.-J.; Wang, K.-Y. Monitoring method of power system wide-band oscillation based on variational mode decomposition and compressive sensing. *Power Syst. Prot. Control.* **2022**, *50*, 63–74. [CrossRef]
53. Mao, X.-B.; Lu, J.-M. AC Sampling Technology of Power Systems Parameters and Its Software and Hardware Designing Methods. *Chin. J. Sci. Instrum.* **2001**, *S2*, 195–196+198. [CrossRef]
54. Song, Q.-Y. Study and Design of SIW Bandpass Filters. Master's Thesis, Xidian University, Xi'an, China, 2010.
55. Zhang, Q.-L. The Study of Low-Temperature Sintered Microwave Dielectric Ceramics and Multilayer Chip Bandpass Filter. Ph.D. Thesis, Zhejiang University, Hangzhou, China, 2004.